

EVALUATING LATENCY IN FIFTH-GENERATION VEHICLE-TO-EVERYTHING COMMUNICATIONS USING ADAPTIVE NEURO-FUZZY INFERENCE SYSTEM MODEL

Hamdy A.M. Sayedahmed^{1,3*}, Emadeldin M. Elgamel^{2,1}, Hesham A. Hefny¹

¹Department of Computer Science, Faculty of Graduate Studies for Statistical Research,
Cairo University, Egypt

²Department of Engineering and Computer Science, Tarleton State University, Texas,
Stephenville, USA

³Department of Information Technology, Central Metallurgical Research and Development
Institute, Giza, Egypt

ABSTRACT

The fifth-generation new radio technology (5G NR) introduces improved functions to the air interface. In addition, the 5G NR non-standalone (NSA) will operate with long-term evolution, enabling vehicle-to-everything communications (V2X) for improved infotainment services. V2X includes four main classes of communications: vehicle-to-vehicle, vehicle-to-infrastructure, vehicle-to-pedestrian devices, and vehicle-to-network. However, the stringent transmission frequency, latency, and throughput requirements of infotainment applications constrain the transmitting packets of 5G-V2X-based NSA in highway scenarios. In this paper, the latency is improved by preventing the physical layer of gNodeB and the user equipment (UE) from sending redundant packets for service in a highway scenario. The proposed approach adopts an adaptive neuro-fuzzy inference system (ANFIS), a powerful modeling technique based on artificial neural networks, and a fuzzy inference system. The performance of ANFIS is compared with that of the traditional 5G V2X NSA architecture in a simulation study using Voice over Internet Protocol (VoIP) traffic. The delays, throughputs, and packet losses of both architectures are determined in radio link control (RLC) and VoIP applications. The switch-modes, signal-to-interference-noise ratios (SINRs), hybrid automatic repeat request (HARQ) error rate, channel quality indicators (CQIs), served blocks, and transmission-state of gNodeB are computed for the two architectures for device-to-device (D2D), uplink (UL) and downlink (DL) traffic directions. The simulation results show comparable SINRs, CQIs, served blocks, and switch modes in both scenarios, but the presented ANFIS model significantly outperforms the traditional architecture in delay by 66% in D2D, 29% in UL, 25% in DL, and packet loss by 21% in UL in RLC, the HARQ error rate by 9% in D2D, 30% in UL, 95% in DL, transmission-state in gNodeB by 29%, and the delay by 4% for UEs, and frame loss by 90% for UE in VoIP.

KEYWORDS

Fifth-generation radio technology, vehicle-to-everything, long-term evaluation, non-standalone

1. INTRODUCTION

The various services of vehicle communications require stringent wireless network infrastructures. The fifth-generation new radio technology (5G NR) introduces promoted functions to the air

interface. 5G NR operates in two modes: standalone (SA) and non-standalone (NSA) [10]. In NSA mode, long-term evolution (LTE) and 5G NR will cooperate to provide high data rates that meet the service requirements of vehicle-to-everything communications (V2X) [7], which include vehicle-to-vehicle (V2V), vehicle-to-infrastructure (V2I), vehicle-to-network (V2N), and vehicle-to-pedestrian (V2P) communications. On the one hand, LTE has high attenuation on highways, insufficient quality of service (QoS), and low resource-allocation behavior in V2V communications [41]. Thus, dedicated-short range communication (DSRC) is essential in such connections [1, 42]. On the other hand, 5G has limited global coverage; and the waveforms and multiple-input multiple-output (MIMO) procedures, of its physical layer signaling, need improvement. 5G NR provides enhanced mobile broadband (eMBB), ultra-reliable low latency communications (URLLC), millimeter-band radios (mmWave), and high data transfer through beamforming [31].

Reducing the delay caused by beamforming and handover in 5G V2X communications (V2V, V2I, and V2N) poses a critical challenge when considering different service requirements [43]. For example, Infotainment applications require a minimum transmission frequency of 1 Hz, a latency of less than 1000 ms, and a throughput of 80 Mbps. In road traffic-flow applications, the minimum transmission frequency, latency, and throughput requirements are 1 Hz, less than 500 ms, and less than 45 Mbps, respectively. In traffic-safety applications, the minimum transmission frequency, latency, and throughput requirements are 10 Hz, less than 100 ms, and less than 700 Mbps, respectively. Finally, autonomous driving applications require a minimum transmission frequency, latency, and throughput of 10 Hz, less than 10 ms, and 5 Mbps, respectively. Achieving these requirements in the presence of DSRC based on IEEE802.11p (in V2V) and LTE (in V2I and V2N) poses difficult problems [6, 21, 32].

5G NR beamforming can be narrowband or wideband. Beamforming allows a sender to direct the transmission in a specific direction toward a vehicle or mobile device, ensuring reliable communications [39]. However, the signal attenuation in highway scenarios exhibits a power-law relationship with sender-receiver distance. This relationship, known as Friis' law, diminishes the effectiveness of beamforming between far-spaced communicating vehicles. Therefore, beamforming is useless in highway scenarios [8].

The delivery and management of beacon messages in highway scenarios require beamforming to convey airframe packets (such as LTE) or handover messages [20, 25]. Airframe messages convey the signal-to-noise ratio, attenuation degree, vehicle speed, and other information. However, as the information changes at millisecond rates, the validity of the information received at the UE/gNodeB is uncertain. To enhance the beamforming performance in such situations, the model used by the vehicle must adaptively learn from anonymous information. Neural fuzzy networks utilize the training and learning algorithms of neural networks to find the parameters of a fuzzy system in uncertain situations. A neural fuzzy network attempts to handle imprecise data and learn from unseen data. In particular, it processes fuzzy logic (which lacks prior knowledge and cannot be learned) with different algorithms and combines their results to obtain the final solution [16].

This work focused on investigating the handover and beamforming issues by considering the delivery of beacon messages using new radio (NR) with LTE in a highway scenario in the 5G V2X environment (V2V, V2I, and V2N). The V2N contains a server that provides simultaneous VoIP to edge users. The main work contribution is to reduce latency during the beamforming and handover processes because of the stringent service requirements of 5G V2X. Also, contributions are summarized as follows:

- (1) Defining ANFIS parameters to enhance the media access control (MAC) and physical (PHY) layers of UE and gNodeB to control beacon packets in the above-described environment.
- (2) A comparison between the adaptive model ANFIS and traditional architecture.
- (3) To improve handover and beamforming in non-standalone 5G V2X issues, most works consider one issue and disregard the other or its effect. In this work, both issues are considered by studying thirteen metrics (delays, throughputs, and packet losses of both RLC and VoIP applications. The switch modes, SINRs, hybrid automatic repeat request (HARQ) error rate, CQIs, served blocks, and transmission state of good)
- (4) In non-standalone 5G V2X, most researchers have not adopted any infotainment service traffic in a highway scenario or core network (V2N). Herein, the VoIP traffic is considered an infotainment service in a highway scenario using a core network.
- (5) Analyzing the ability of the adaptive model on handover and beamforming to achieve the 5G V2X service requirements.

The remainder of the paper is organized as follows. Section 2 reviews the related work and Section 3 introduces the ANFIS model as an adaptive model for solving the learning problem. Section 4 presents the model flow and uncertainty management of the ANFIS model. The experimental environment and results are discussed in Section 5 Finally, Section 6 concludes the paper.

2. RELATED WORK

Despite 5G V2X will be launched in NSA mode depending on V2V, V2I, V2P, and V2N in various road types (urban, rural, or highway) with different traffic types. Many researchers have investigated the performance of 5G V2X in NSA mode using one or two V2X network types without considering highway scenarios and VoIP traffic. Attempts to improve the packet loss, delay, and throughput have been variously reported. The research objectives of earlier works are summarized below:

- (1) 5G performance evaluations of data delivery using a V2V network [4-5, 35]
- (2) Evaluations of delay, throughput, and packet loss in 5G using V2V and V2I with multi-access edge computing (MEC) [26, 30]
- (3) 5G performance evaluations of V2V and V2I without MEC or a core network [12] [27-29]
- (4) Evaluations of 5G scheduling schemes using V2V and V2I [2,9]
- (5) Measurements of theoretical routing performance in 5G using V2V and V2I [14]
- (6) Network-slicing enhancement in 5G using V2V and V2I [40]

To enhance the NSA mode in 5G, researchers have recently improved the beamforming [18-19, 22], handover [3,11,15], or beamforming with handover [34]. However, to our knowledge, no 5G V2X evaluations in NSA mode in the V2V, V2I, and V2N environments of a highway scenario with VoIP applications have employed adaptive neural fuzzy neural models, which can simultaneously consider both beamforming and handover.

Nevertheless, various works have investigated concurrent beamforming and handover. For example, the authors of [34] presented an adaptive beamforming method for highway wireless handover based on a theoretical analysis, which considers beacon messages only. Mathematical analysis of handover can improve the delay in 5G V2X communications [3]. Hussain et al. 2021 [11] enhanced the throughput, delay, and packet loss during the handover process using a Q-learning algorithm and fuzzy logic. Liu et al. [15] presented a fuzzy model that improves the handover in 5G

communications. Meanwhile, vehicle movement prediction based on global positioning systems (GPSs) and DSRC beacon messages can relieve the beamforming overhead [18]. Prathiba et al. [22] proposed a software-defined network (SDN) based on machine learning for beamforming broadcasting–safety messages. Their software improved the latency of the delivery ratio. Finally, Mezzavilla et al. [19] introduced a statistical beamforming method that accurately controls the transmission direction. Table 1 compares the features of our presented model and related works focused on beamforming or handover.

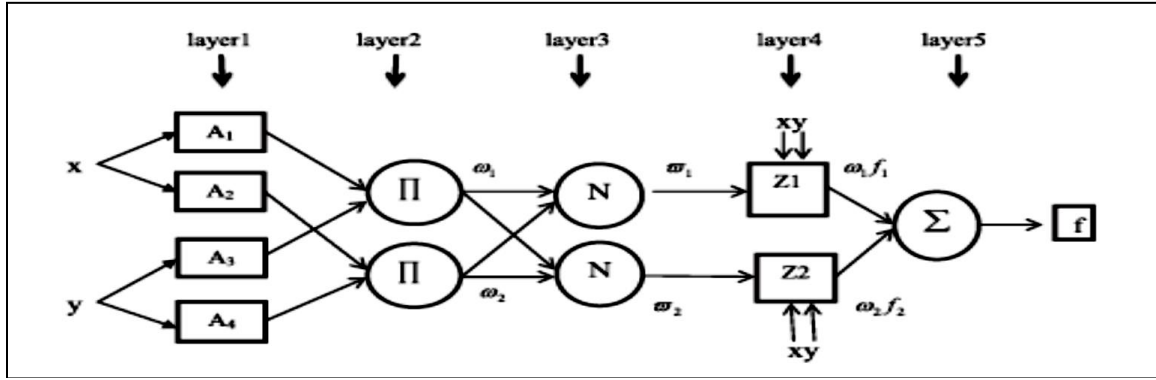


Figure 1. A typical architecture of the adaptive neuro-fuzzy inference system with two inputs, and one output

Table 1: Feature comparison of the proposed method and related work

Ref.	Method	Evaluation mode	Road type	5G Mode	Network type	Beamforming	Handover
[18]	Based on GPS	Mathematical analysis	4-Lanes	Non-Standalone	V2V, V2I		
[19]	Statistical analysis	Statistics	Urban, rural	Non-Standalone	V2V, V2I	√	
[22]	SDN and machine learning	Performance evaluation	Highway	Standalone	V2V, V2I		
[3]	Mathematical analysis	Analysis	Urban	Standalone	V2V, V2I		
[11]	Q-learning and fuzzy logic	Performance evaluation	Urban	Non-Standalone	V2V, V2I		√
[15]	Fuzzy model	Numerical analysis	Urban	Standalone	V2V, V2I		
[34]	Mathematical analysis	Analysis	Highway	Non-Standalone	V2V, V2I	√	√
This work	Adaptive neural fuzzy model	Performance evaluation	Highway	Non-Standalone	V2V, V2I, V2N	√	√

3. ARCHITECTURE OF THE ANFIS MODEL

The ANFIS model, originally called the adaptive network-based fuzzy inference system [36], utilizes the learning strength and fine-tuning of the membership function to check linguistic terms and numeric facts. It then derives the fuzzy IF-THEN rules with suitable membership functions attained from training pairs. Figure 1 shows a typical architecture of the ANFIS model with two inputs and a single output [37].

The ANFIS model consists of five layers as follows:

1) Layer-1: every neural node i in this layer is a membership function expressed:

$$O^1_i = \mu_{A_i}(X) \quad i=1,2,3,\dots \quad (1)$$

where x is the input to node i , A_i is a fuzzy set representing a linguistic term in a node function, and O^1_i is the value of the membership function.

2) Layer-2: every node in this layer calculates the product operation by Equation (2). The output is called the firing strength of the rule.

$$O^2_i = \omega_i = \mu_{A_i}(X) * \mu_{B_i}(Y) \quad i=1,2,\dots \quad (2)$$

3) Layer-3: the nodes at this layer are fixed for evaluating the normalized firing strength (ratio of the i th rule's firing strength to the sum of all rules' firing strengths) as follows:

$$O^3_i = \bar{\omega}_i = \frac{\omega_i}{\omega_1 + \omega_2} \quad i=1,2,\dots \quad (3)$$

4) Layer-4: the nodes in this layer are adaptive for calculating the output of layer 3 in terms of the parameters (p, q, r).

$$O^4_i = \bar{\omega}_i F_i = \bar{\omega}_i (p_i X + q_i Y + r_i) \quad i=1,2,\dots \quad (4)$$

Where $\bar{\omega}_i$ is the output of layer 3, and (p_i, q_i, r_i) is the parameter set. Parameters in this layer will be referred to as consequent parameters.

5) Layer-5: is a single fixed node that sums the overall outputs as:

$$O^5_i = \sum_{i=1}^n \bar{\omega}_i F_i \quad i=1,2,\dots,n \quad (5)$$

The ANFIS model accepts sharp values as inputs to be fuzzified in layer-1. These values pass through the inference process in layers 2 and 3, which apply fuzzy rules. The output of each corresponding rule is computed in layer-4. Finally, all outcomes from layer-4 are summed to obtain a single result in layer-5. The ANFIS model is a Takagi Sugeno -type fuzzy inference system that can adjust the forms of the fuzzy membership functions of the fuzzy IF-THEN rules. Applying a learning algorithm to input-output datasets, it then constructs a highly accurate mapping from input space to output space. The ANFIS model shown in Fig. 1 is described by the following fuzzy IF-THEN rules:

Rule 1: IF x is A_1 and y is A_3 Then $f_1 = p_1 x + q_1 y + r_1$

Rule 2: IF x is A_2 and y is A_4 Then $f_2 = p_2 x + q_2 y + r_2$

where: A_1 and A_2 are the fuzzy linguistic values of input x , A_3 and A_4 are the fuzzy linguistic values of input y , f_1 and f_2 are a linear combination of inputs with constant terms, p_1 , q_1 , and r_1 are the parameters of the first linear combination f_1 , and p_2 , q_2 , and r_2 are the parameters of the first linear combination f_2 .

The ANFIS parameters are optimized by a hybrid algorithm that combines the least squares estimate and the gradient descent method [36]. During the training process, the parameter optimization process continues until the error between the target and the actually obtained output is minimized [37].

4. UNCERTAINTY MANAGEMENT AND MODEL FLOW

In this paper, the ANFIS model was selected for 5G V2X enhancement in NSA mode. Moreover, the Gaussian function is selected as the membership function because its small number of parameters (two parameters) helps to reduce the computational complexity. The environment consists of hybridized NR and LTE communications which allow the exchange of several types of beacon packets. Herein, the ANFIS requires rational actions of the sender's MAC and PHY layers when sending/receiving beacon packets such as LTE airframes. For example, in a highway scenario, UEs require more beacon packets [38] to achieve their goal (informing dangerous situations or demanding infotainment services), either because the UE distribution is uneven or the signal is attenuated. When the signals weaken, the number of beacon messages or the delay lengthens. The signal quality is reduced by factors such as carrier band, received power, traffic direction (uplink/downlink), gains of the transmitted and receiving antennas (TX and RX, respectively), cable loss, attenuation (path loss and shadowing), speed, thermal noise, attenuation fade, sender-receiver distance, and noise figure. The noise figure is affected by the input signal level. To reduce the delay, some studies relate these parameters to the degree of signal quality. Meanwhile, datasets have been scanned using different unsupervised learning algorithms such as the k-nearest neighbor algorithm [33] and hierarchical clustering [13] to optimize the number of clusters. These assessments, along with the method in [24], have confirmed three effective parameters: received power, attenuation, distance, and antenna gain.

ANFIS exploits the uncertainty in the input parameters to enhance the signal quality and reduce the network overhead caused by feedback packets, thus increasing the UE's signal strength. More specifically, ANFIS enables rational decision-making by UEs sending responses/requests through LTE airframe beacon messages. For this purpose, ANFIS utilizes the received power, attenuation, distance, and antenna gain inputs of the UE. Figure 2 is a flowchart of the ANFIS training procedure before sending the LTE airframe, feedback, or regular packet in the uplink, downlink to gNodeB, or UE to UE. A UE/good checks its status in terms of four parameters: received power, attenuation, distance, and antenna gains. Typically, these parameters change on millisecond timescales and their values can be theoretically calculated using Equations (6), (7), and (8). The power received by the UE is changed by many factors, including the antenna gains [27]. As the attenuation is affected by path loss, it should be equal along the non-line of sight and line of sight at any given distance [17]. Unfortunately, the distance between the UE and gNodeB is difficult to measure because the vehicles can stop and accelerate in a highway scenario.

The received power and path loss are both affected by distance. The antenna gains vary with position and weather conditions [23]. The UE's parameters are normalized in the range [0,1]. When fired with

the knowledgebase (IF-THEN rules), the UE will send its packet or wait. The ANFIS creates an arrangement pattern of sending and receiving packets that allow reliable communications among the UE/gNodeBs. UEs with undesired status are prevented from engaging the channel and causing interference. The power at the receiving antenna is calculated as

$$P_r = \frac{P_t G_t G_r \lambda^2}{(4 \pi d)^2} \quad (6)$$

where P_t and G_t are the output power and gain of the transmitted antenna, respectively, G_r is the gain of the receiving antenna, λ is the wavelength, and d is the distance between the antennas. The path loss (in db) is determined as

$$PL_{(db)} = 20 \log_{10} \left(\frac{4 \pi d}{\lambda} \right) \quad (7)$$

where d is the sender-receiver distance. Finally, the antenna gain is given by

$$G = \frac{4 \pi A_e}{\lambda^2} \quad (8)$$

A_e is the effective area of the signal.

To cope with the uncertainty and dynamicity of learning the four parameters, we employ an adaptive neural fuzzy network. The uncertainty is handled by the fuzzy part, which applies "degrees of truth" rather than the discrete outcome (true–false or 1–0) in conventional computing. Meanwhile, the neural network part is responsible for adapting unknown learning patterns. The adaptive neural fuzzy network model is based on a knowledgebase and learning algorithms that provide low-cost approximate solutions to lower the delay. The model infers an approximate reasoning decision from inexact knowledge (received power, attenuation, distance, and antenna gain) and unknown patterns to ensure reliable connections.

In this study, four inputs (received power, attenuation, distance, and antenna gain), one output (noise figure), and an inference system consisting of 81 rules construct the basic model. For each input and output, three membership functions – linguistic terms- covers each input and output universe of discourse, and the selection of membership function type significantly affects the model behavior. Also, The consequent parameters (p_i , q_i , r_i) determine the membership function that requires computing the root mean square error (RMSE) for training data.

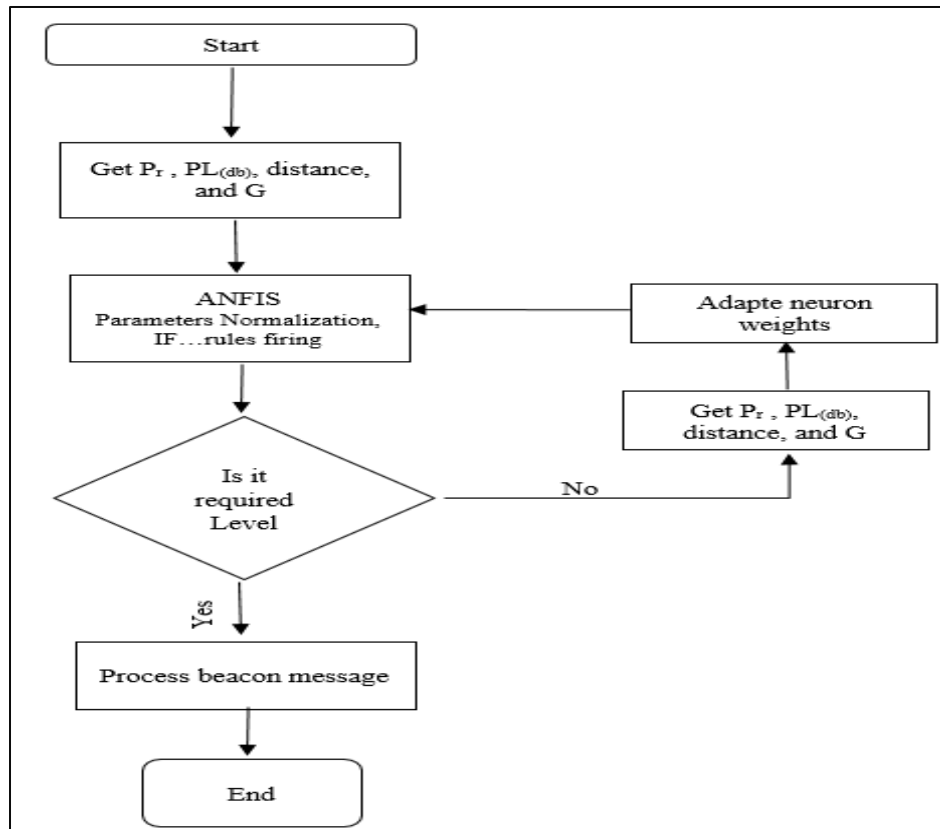


Figure 2. Flowchart of the ANFIS training procedure

5. MATERIAL AND METHODS

5.1. Environmental Setting

We combined Objective Modular Network Test bed in C++ (OMNET++) 6.0 with Simu5G 1.1, Internet networking (INET) 4.3, Veins 5.0 frameworks, and Simulation of Urban Mobility (SUMO) simulator 1.8. OMNET++ is an open-source discrete-event simulation environment that can model wireless communication. The Simu5G framework can model 5G new radio access and the INET framework can provide protocols, agents, and other network models. The Veins' framework based on OMNET++ and SUMO (a road traffic simulator) offers inter-vehicle communication models. The ANFIS model is obtained from MATLAB 2020a “adaptive neural fuzzy network toolbox.” The traditional architecture (TA) and the ANFIS model were evaluated in different 5G V2X scenarios under previously described environmental settings [9, 12, 14, 27-29]. The first scenario uses the TA and the second uses the ANFIS model with an acceptance condition of less than three for the noise figure. The comparison includes the device-to-device (D2D), uplink (UL), and downlink (DL) connections. Table 2 shows the main settings of both scenarios.

Table 2. Environmental settings of the two scenarios in the present study

Simulation Parameter	Value
Simulation time	10 min.
Area	20000 m ²
Communication type	5G V2X, LTE, DSRC
Road type	Highway
No. of Servers	1
Traffic type	VoIP
No. of gNodeB	2
Thermal noise	-104.5 dBW/Hz
Cable loss	2 dB
No. of lanes/length	4/4 km
No. of Vehicles	15
Velocity of vehicle	Range [0, 100] km/h
Acceleration	2.9 km/h
Mobility model	Linear mobility
Carrier frequency	[2, 6] GHz
No. of Bands	25
UE Tx Power	26
eNodeB Tx Power	46

5.2. Environmental Results and Discussion

The performances of the ANFIS model and TA were evaluated in terms of thirteen performance metrics in the two scenarios. The results are shown in Figures 3–15 and discussed below.

RLC is a data link layer in UEs and gNodeB, that frames the data into several chunks of a specified size and passes them one by one. The RLC forms part of the air interface control and user planes in LTE and 5G. It transfers the upper-layer protocol data units (PDUs), error correction through automatic repeat requests (ARQs), duplicate detection, protocol error detection, and recovery services. In addition, the RLC delay measures the travel time of fragments from UEs to gNodeBs or gNodeBs to UEs. The UEs using ANFIS outperformed those using the TA. Because the ANFIS acceptance condition depends on the noise figure, a UE blowing the accepted state waits until its received power, attenuation, distance, or antenna gain changes to the transmit state. Therefore, ANFIS limits the transmitted beacon packets (LTE airframes) from UE to gNodeB in the UL direction and reduces the number of duplicate packets, error detection, and recovery services in the device-to-device (D2D) links. Further more, ANFIS in gNodeB prevents the gNodeB from transmitting packets to a far or weak signal UE in the DL connection. As shown in Figure 3, ANFIS reduces the average RLC delay from that of TA in D2D, UL, and DL communications.

RLC throughput measures the number of successfully sent chunks from UEs to gNodeB or gNodeB to UEs in a given time. Therefore, reducing the number of fragments will increase the probability of success in the transmitted data because few pieces require less sending time than many pieces. In general, the UEs using ANFIS produces lower throughput than TA because ANFIS adaptively learns the UE's received power, attenuation, distance, and antenna gain; and updates its neural network weights. The time of adjusting the ANFIS weights in UE/ gNodeB increases due to constraints on the received/transmitted packets. In D2D, ANFIS reduces the throughput from that of TA by decreasing

the number of received/sent packets from UE to UE. In UL and DL, a UE cannot send/receive a packet to the gNodeB unless its antenna gain satisfies the ANFIS, so the number of packets and throughput are both reduced. As shown in Figure 4, ANFIS reduces the average RLC throughput from that of TA in D2D, UL, and DL communications.

RLC packet loss measures the number of transmitted packets that fail to arrive at their destination. When a destination cannot receive a transmitted fragment, an error correction through the automatic repeat request (ARQ) service in NR RLC is triggered. ANFIS reduces the number of transmitted fragments because it depends on the received power, attenuation, distance, and antenna gain. ANFIS decreases the probability of triggering the ARQ service, thus affecting packet loss. In UL, the UEs begin sending packets to the gNodeB but because the UE states can change, increasing the packet sending in TA increases the packet loss. In contrast, the UEs using ANFIS incur lower packet losses because they reduce the number of ARQ invocations and duplicate detection services in RLC. In DL, the gNodeB state does not change and the gNodeB learns the UE states from the UL. Therefore, the DL packet losses in ANFIS and TA are similar. Furthermore, ANFIS allows a UE to know and update the current states of other UEs. Therefore, the learning process prevents packet loss in the D2D link direction. As shown in Figure 5, ANFIS reduces the average RLC packet loss from that of TA in UL and obtains similar packet loss to TA in D2D and DL.

A **PDU** is a singular information unit transmitted among peer ends. Therefore, the NR RLC PDU is an intensified service data unit (SDU) shared segment, and the NR RLC PDU delay measures the travel time of each fragment between UEs to gNodeBs or gNodeBs to UEs. As the RLC delay is lower in ANFIS than in TA, the UEs using ANFIS outperform those using TA in PDU delay. When an end (UE/gNodeB) receives a fragment, it checks its status based on the noise figure. If the signal quality is equal to or below the specified condition, the end obtains the fragment; if not, it drops the fragment. As the sender performs equivalently to the receiver, the signal quality is high on both sides and the fragment is transmitted accurately with low latency. In the UL and DL, the ANFIS reduces the number of ARQs in the SDU segments, thereby reducing the delay of each segment. Similarly, in D2D, no UE can connect to any other UE unless the noise figure is acceptable. As shown in Figure 6, ANFIS reduces the average RLC PDU delay from that of TA in D2D, UL, and DL communications.

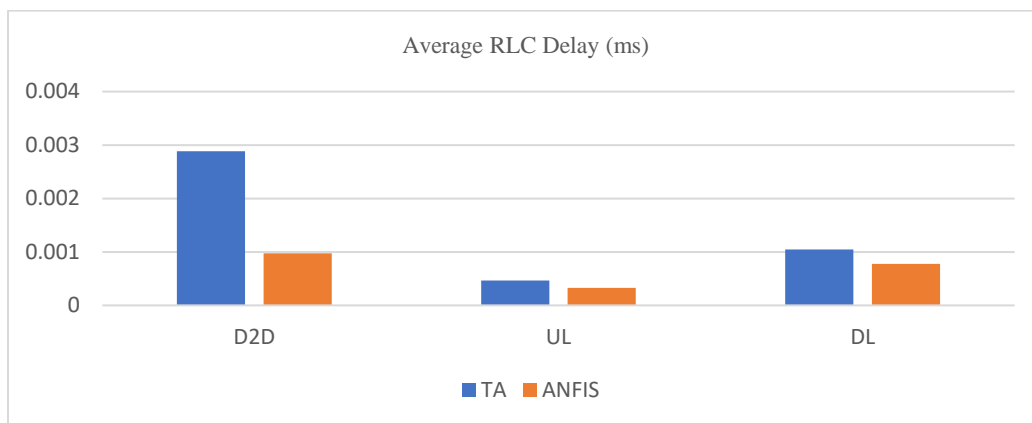


Figure 3. Average radio link control (RLC) delays in D2D, UL and DL communications

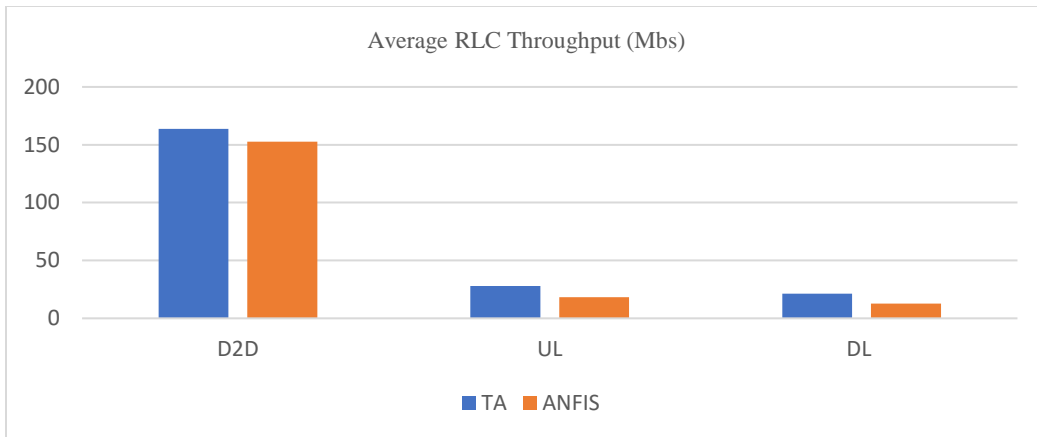


Figure 4. Average RLC throughputs in D2D, UL and DL communications

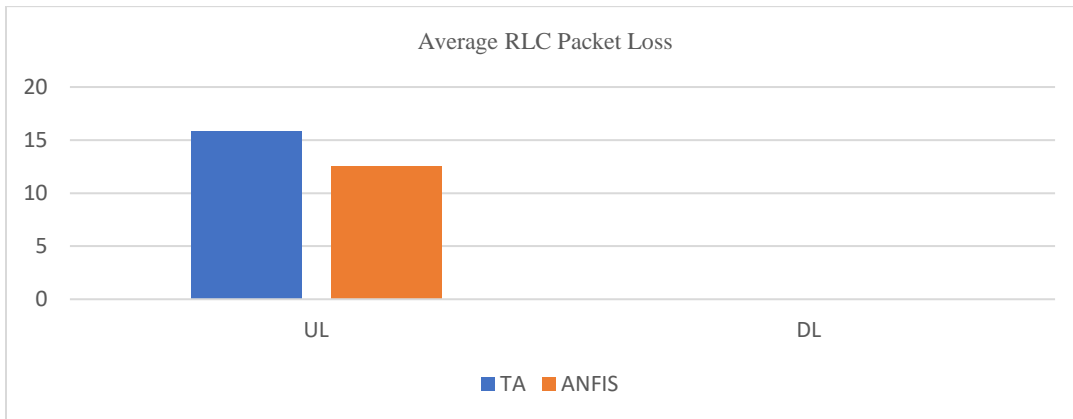


Figure 5. Average RLC packet losses in D2D, UL and DL communications

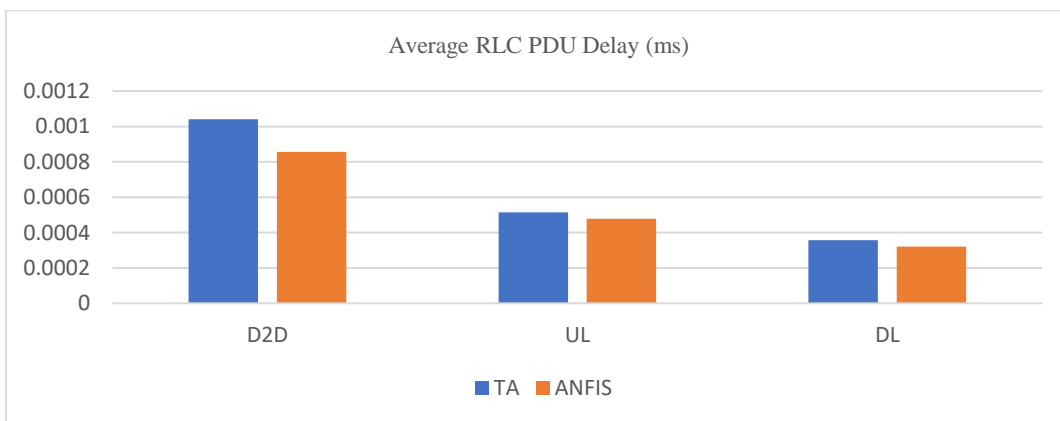


Figure 6. Average RLC protocol data unit (PDU) delays in D2D, UL and DL communications

Hybrid Automatic Repeat Request (HARQ) combines ARQ with forward error correction (FEC). When a sender receives no acknowledgment (ACK) before timeout, it re-transmits the package

assuming that the receiver has discarded the bad packet. The HARQ error rate measures the number of bad packets. Recall that ANFIS processes fewer transmitted/received packets than the TA; therefore, fewer packets reach their destinations before the timeout and more acknowledgments (ACKs) are returned to the sender. Consequently, ANFIS lessens the need for ARQs and reduces the FEC and HARQ error rates in D2D, UL, and DL communications. Figure 7 compares the average HARQ error rates in D2D, UL, and DL using ANFIS and TA.

In 5G, the **SINR** is a measure of signal quality. Specifically, it measures the strength of the desired signal over the undesired interference and noise. Measured in decibels, the SINR increases with increasing signal quality. Signal interferences include multiple access interference, channel interference, and adjacent channel interference. In the highway scenarios of the present study, the signal interference on UEs is low, so the SINRs are similar in ANFIS and TA. In D2D, the UEs move in sequence through the lanes with no redundant packets in transmitting/receiving. Such linear movement diminishes the SINR in both model architectures. In UL and DL, the UEs move either parallel or perpendicular to the good, which is fixed in position. Here, the behaviors of ANFIS and TA are similar because the UEs maintain beam forming to the gNodeB (see Figure 8).

CQI is a measure of the channel quality from UE to good. This indicator assigns the level of modulation and coding operated by the UE. The CQI performances of ANFIS and TA are comparable as the UE trajectory is the same in both cases. However, as the CQI measures the signal quality from UE to good, there are no results for D2D links. On the UL and DL sides, ANFIS mainly relies on the received power, attenuation, distance, and antenna gain to improve the noise figure. A good noise figure leads to high signal quality. As the mobility of the UEs is the same in both scenarios, ANFIS exerts a slightly lower effect than the TA and outperforms the TA because it depends on signal quality and reduces the duplicated and unnecessary data, as shown in Figure 9.

When incorporated with 5G, LTE provides four modes (called **switch modes**) for each pair of UEs in a switch list. The switch mode time defines the average time in which a UE notifies other UEs that it has switched. This simulation omits the UL and DL and considers D2D communications only. The switch mode is taken as a measure of UE handover time. The UEs behave similarly in both cases because the trajectory of the UEs is identical. Each EU is handed over by the nearest good, whose position is fixed in both scenarios. Therefore, TA and ANFIS achieve similar average switch mode times of all UEs in D2D communications (Figure 10).

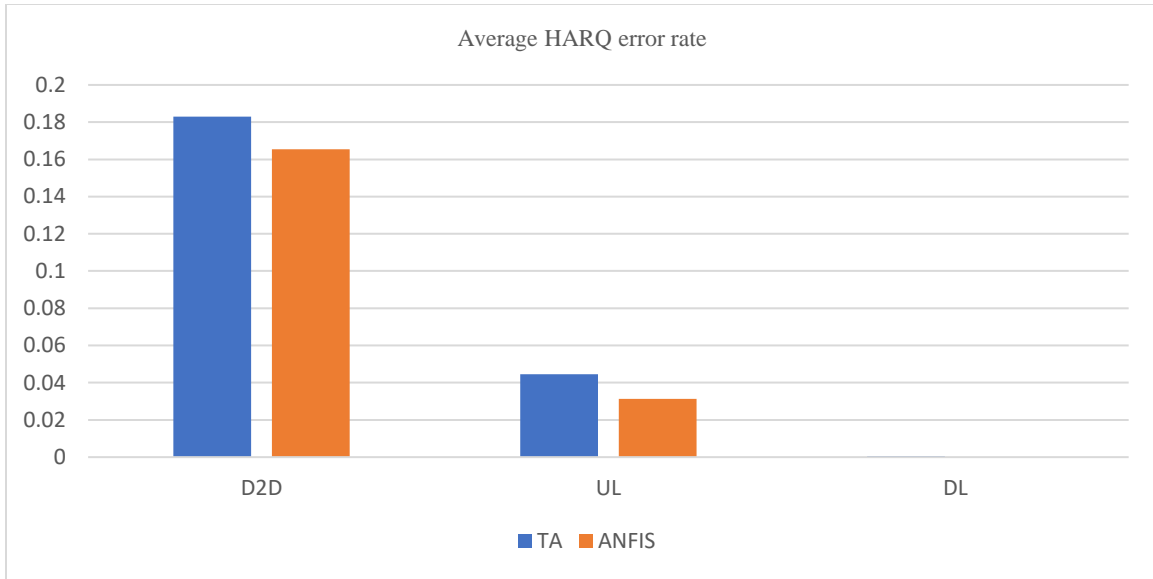


Figure 7. Average HARQ error rates in D2D, UL and DL communications

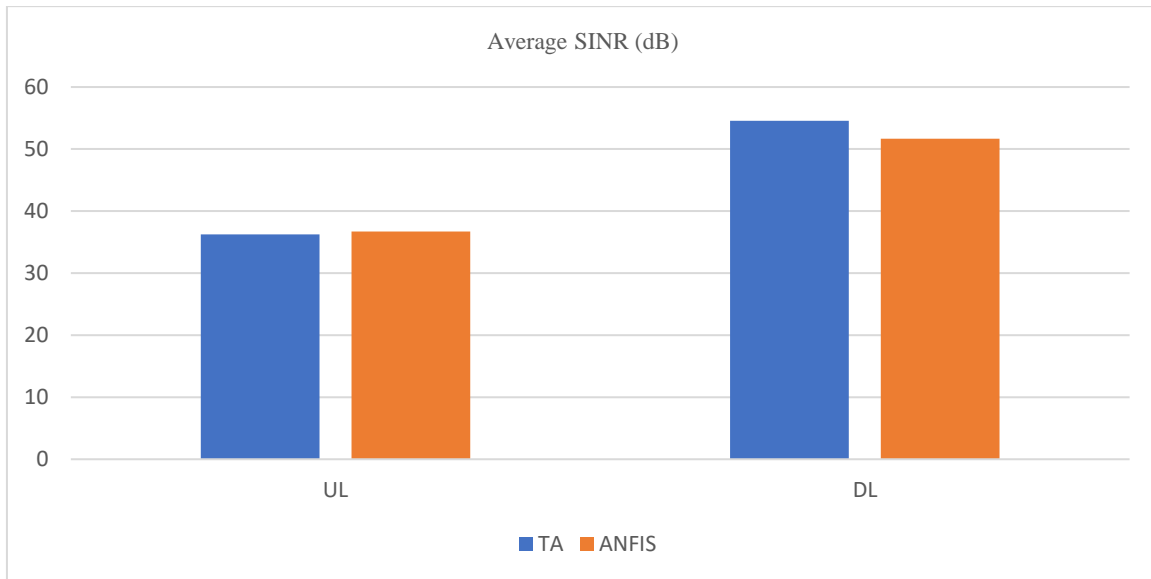


Figure 8. The Average SINR in UL and DL communications

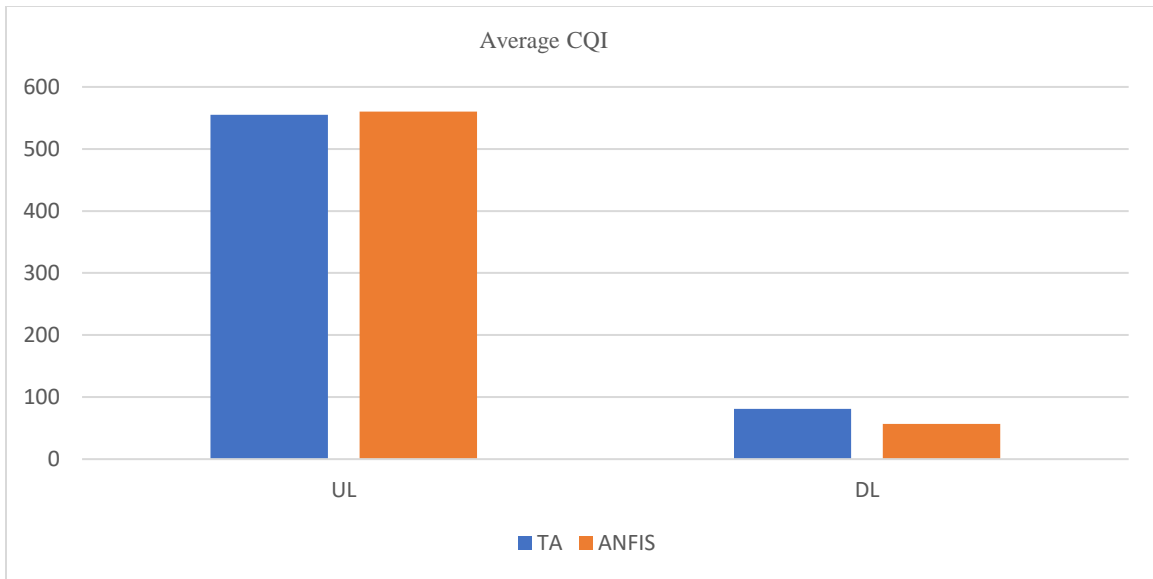


Figure 9. Average CQIs in UL and DL communications

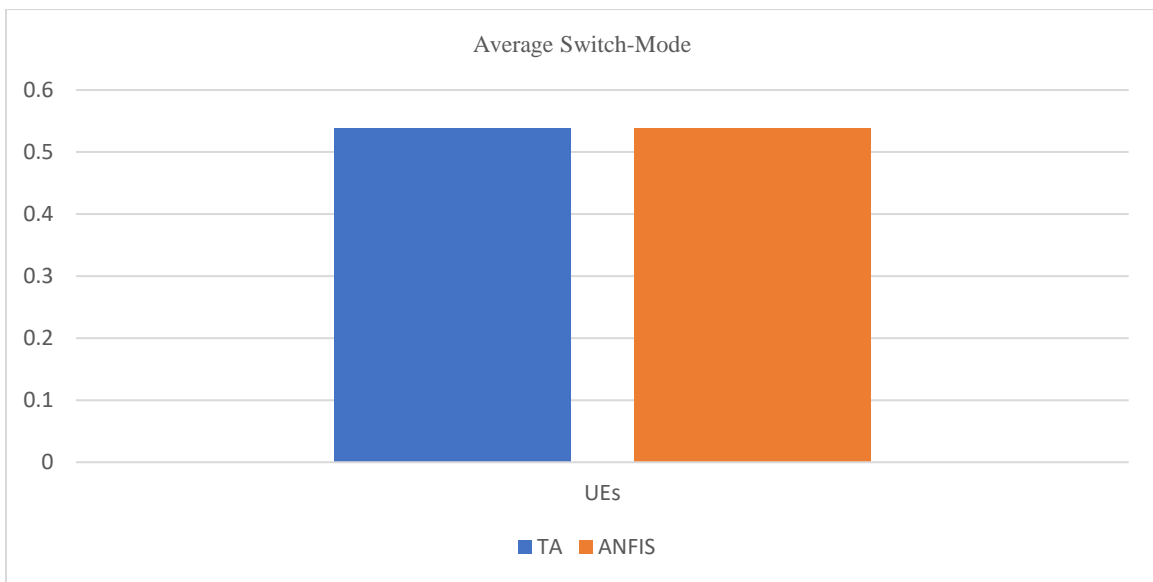


Figure 10. Average switch-mode times of the UEs using ANFIS and TA in D2D communications

Average served blocks define the number of operated blocks scheduled for UL and DL data transmission in a gNodeB. In UL or DL communications, ANFIS in the physical layer of gNodeB prevents the gNodeB from receiving blocks that violate the acceptance condition. Therefore, a gNodeB using ANFIS serves more blocks than a gNodeB using TA while retaining the quality of the VoIP service, as discussed for the following metrics. ANFIS limits the number of transmitted/received packets from gNodeB to UE; in particular, it prevents the gNodeB from sending packets to a far or weak signal UE. As shown in Figure 11, ANFIS raised the average number of served blocks from that of TA.

The transmission-state average time is the time over which a gNodeB transmits a service from a server to a UE. In other words, it determines the speed of service to a UE. ANFIS reduces the average gNodeB transmission-state time from that of TA because the number of requested UEs is restricted by the ANFIS condition (see Figure 12). Therefore, ANFIS reduces the number of packets received from the UEs and hence the wait time of the schedule.

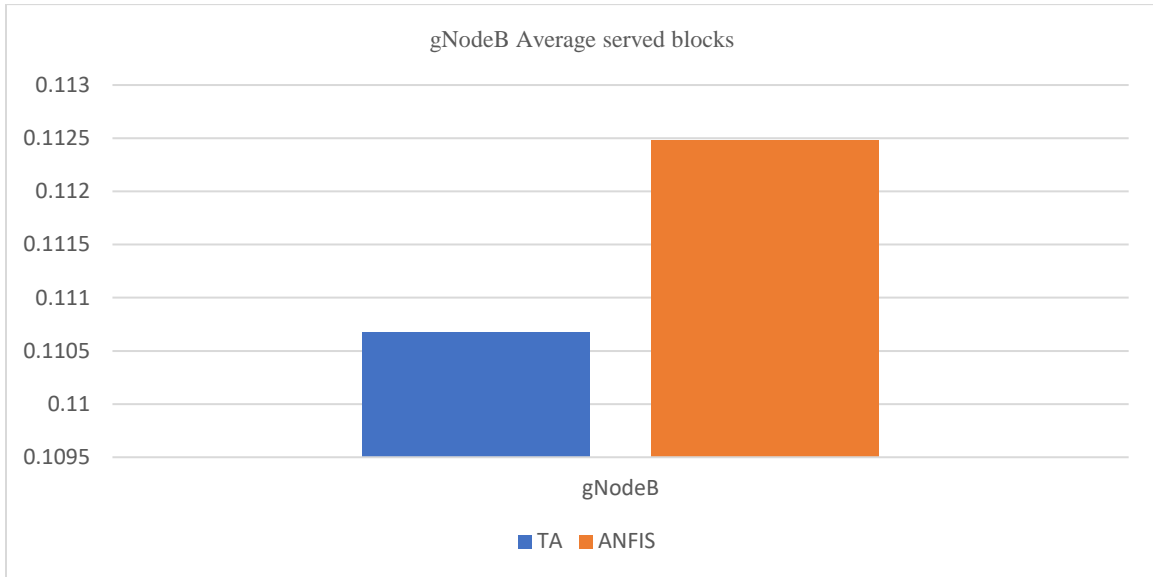


Figure 11. Average served blocks in gNodeB

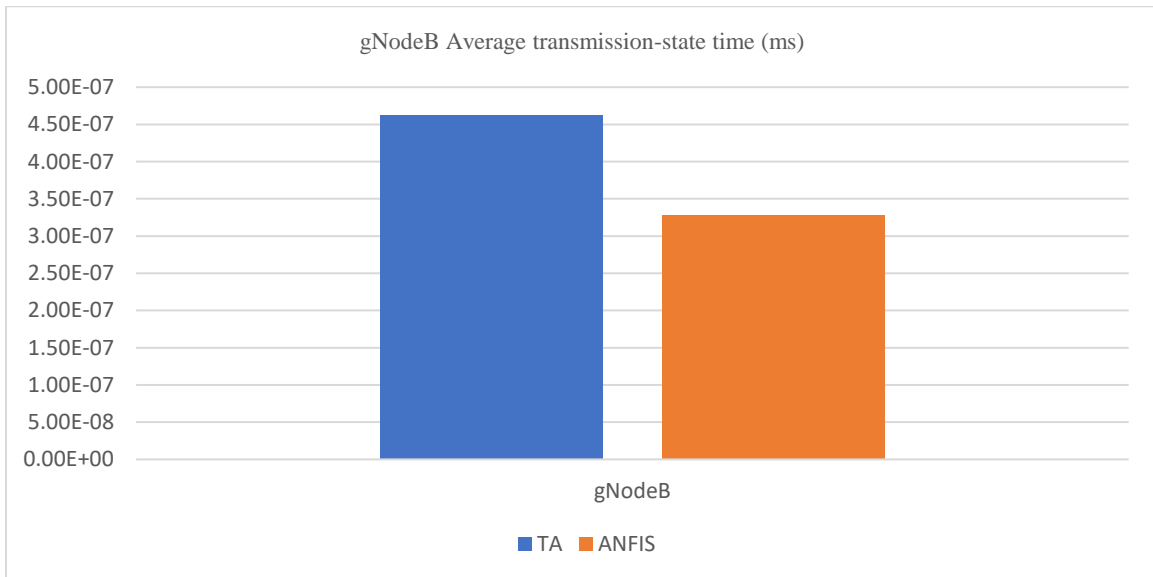


Figure 12. Average transmission-state time in gNodeB

Besides the UE and good metrics, we define three metrics that measure the effects of ANFIS and TA on VoIP applications. These metrics are the **VoIP frame delay**, measures the average wait time for frames.

The **VoIP frame throughput**, which measures the number of successful frames in a given time. **VoIP frame loss**, which represents the number of lost frames. The VoIP frame delay is directly affected by the RLC PDU delay (in D2D, UL ,and DL) and the transmission-state time. As ANFIS outperforms the TA on both of these metrics, it lowers the VoIP average frame delay from that of TA for UEs (see Figure 13).

Figure 14 compares the average VoIP frame throughputs of all UEs using ANFIS and TA. Because ANFIS constrains the number of received/transmitted packets, it lowers the throughput. In contrast, the TA by default increases the number of received/sent packets from the UE directing the throughput; therefore, the UEs using TA present higher VoIP average throughput than UEs using ANFIS.

Figure 15 compares the VoIP frame losses of the UEs using ANFIS and TA. The number of lost frames increases when the number of frames grows large, when the good schedule or links are busy, or when the signals are weak. ANFIS organizes the gNodeB schedule and exploits the high-valued signal strengths to reduce the number of processed frames and facilitate transmission at UE/gNodeBs. Consequently, UEs using ANFIS lose fewer frames than UEs using TA.

The results clarify that in general, ANFIS assists the UE to UE, UE to gNodeB, and gNodeB-to-UE transfer in VoIP applications; meanwhile, the signal quality constraints ensure the high quality of the transfers.

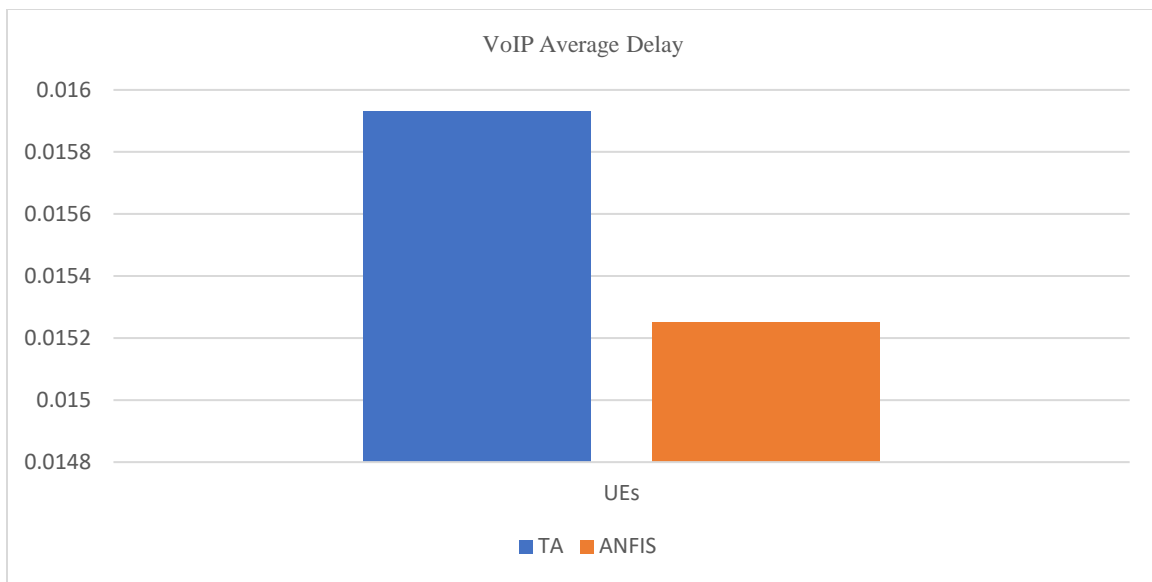


Figure 13. Average VoIP delays

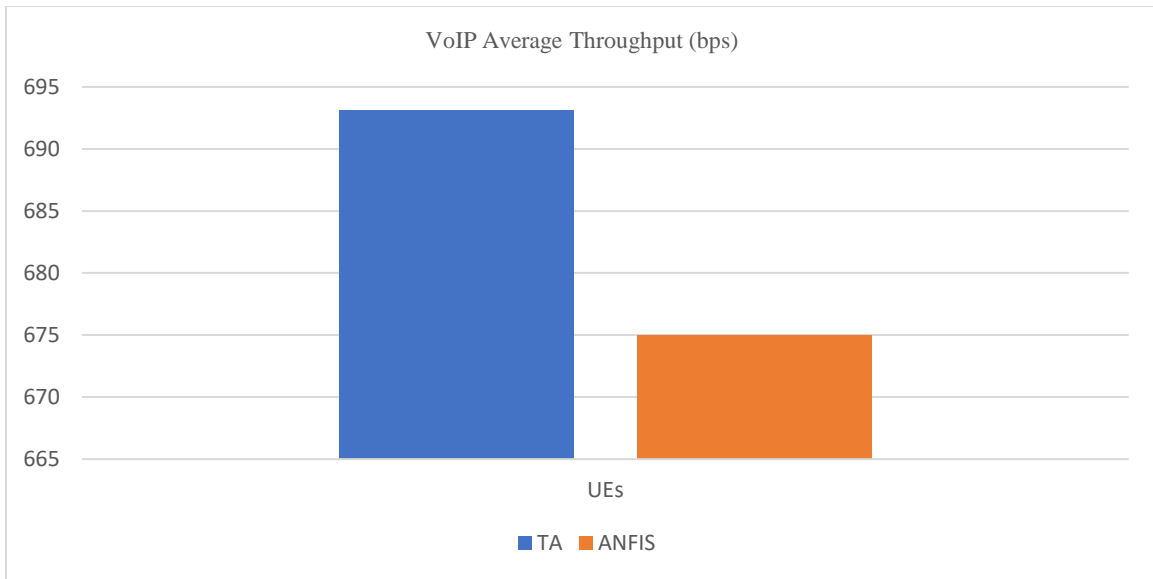


Figure 14. Average VoIP through puts

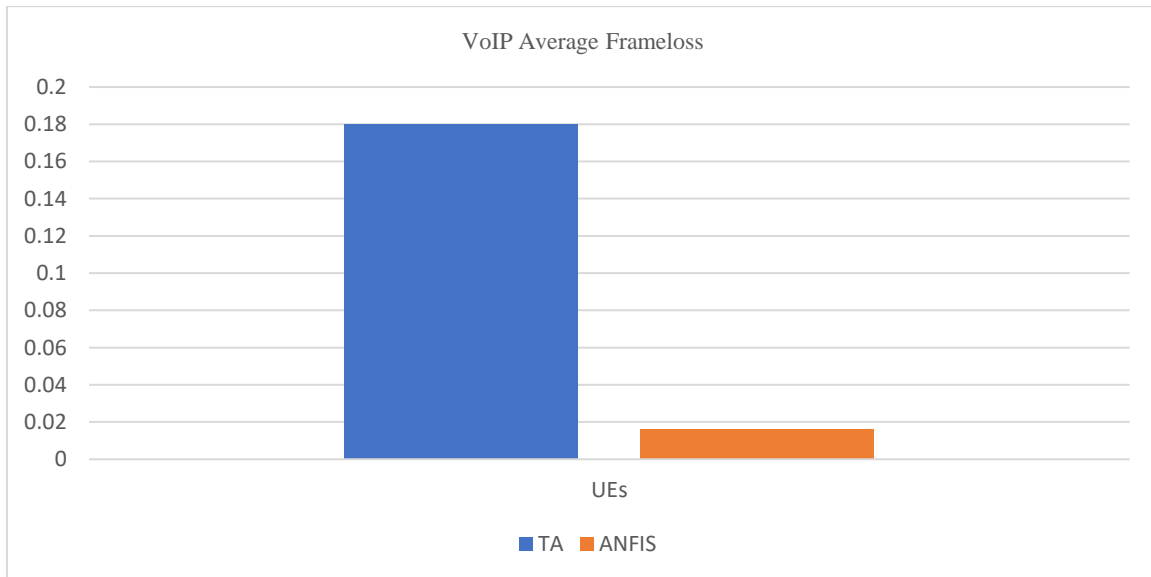


Figure 15. Average VoIP frame losses

6. CONCLUSION

This paper presented an ANFIS model for controlling the MAC and PHY layers in gNodeB and the UEs in NSA 5G V2X. Before broadcasting messages, the UE/gNodeB checks whether its status satisfies the ANFIS condition. If the UE/gNodeB's status is within the allowable threshold of ANFIS, the message is processed; otherwise, the message is dropped and the UE/gNodeB waits. Consequently, ANFIS reduces the number of processed messages.

We compared the performances of our proposed neural fuzzy network model and the TA in a highway NSA 5G V2X application with VoIP traffic using Simu5G, INET, and Veins frameworks, along with the OMNeT++ and SUMO simulators for 5G V2X and the MATLAB R2020a ANFIS toolbox. The first scenario adopted the standard NSA 5G V2X architecture; the second scenario employed the ANFIS model. In thirteen experiments, we measured the delay, throughput, and packet loss of RLC, the switch mode, SINR, HARQ error rate, CQI, served blocks, and transmission state of good and the delay, throughput, and frame loss of VoIP.

ANFIS organizes the sending/receiving of beacon messages between each communicating pair (UE/gNodeB, UE/UE, or gNodeB/gNodeB). This arrangement improves the signal quality because the channel is free, does not affect the handover process (as shown by the switch mode metric), and little affects the beam forming (as demonstrated by the SINR metric). In general, ANFIS is more suitable than the TA in fast UEs such as highway scenarios.

The simulation and evaluation of ANFIS required intensive computational resources and much effort for synchronizing the frameworks (Simu5G, Veins, and INET) with the OMNET++ and SUMO simulators. Moreover, a numerical comparison between the ANFIS and previous works was precluded by a lack of implementation steps in previous publications. In future work, we will add factors and metrics in the ANFIS to enhance its SINR, CQI, and switch-mode decision-making.

CONFLICT OF INTEREST

The authors declare no conflict of interest.

REFERENCES

- [1] K. Abboud, H. A. Omar, and W. Zhuang. "Interworking of DSRC and cellular network technologies for V2X communications: A survey." *IEEE trans. Veh technol* 65, 9457-9470, July, 2016.
- [2] R.V. Akhpashev, V.G. Drozdova, "The 5G new radio scheduler efficiency investigation for remotely distributed V2X entities", in: *International Multi-Conference on Industrial Engineering and Modern Technologies (FarEastCon)*. IEEE, pp. 1–4, December, 2020.
- [3] I.A. Alablani, M.A. Arafah, "Applying a dwell time-based 5G V2X cell selection strategy in the City of Los Angeles, California", *IEEE Access* 9, 153909–153925, November, 2021.
- [4] W. Anwar, N. Franchi, G. Fettweis, "Physical layer evaluation of V2X communications technologies: 5G NR-V2X, LTE-V2X, IEEE 802.11bd, and IEEE 802.11p", in: *90th Veh. Technol. Conference (VTC2019-Fall)*,. IEEE, pp. 1–7, September, 2019.
- [5] T. Bey, G. Tewolde, "Evaluation of DSRC and LTE for V2X", in: *9th Annual Computing and Communication Workshop and Conference (CCWC)*. IEEE, pp. 1032–1035, March, 2019.
- [6] M. Boban, A. Kousaridas, K. Manolakis, J. Eichinger, W. Xu, "Connected roads of the future: use cases, requirements, and design considerations for vehicle-to-everything communications", *IEEE Veh. Technol. Mag.* 13, 110–123, September, 2018.
- [7] E. Dahlman, S. Parkvall, J. Skold, "5G NR: the Next Generation Wireless Access Technology", 2nd ed., Academic Press, ch, 2–4, 2020.
- [8] M. Giordani, A. Zanella, M. Zorzi, "LTE and millimeter waves for V2I communications: an end-to-end performance comparison", in: *89th Veh. Technol. Conference (VTC2019-Spring)*. IEEE, pp. 1–7, June, 2019.
- [9] B. Guo, X. Zhang, Y. Wang, H. Yang, "Deep-Q-network-based multimedia multi-service QoS optimization for mobile edge computing systems", *IEEE Access* 7, 160961–160972, November, 2019.
- [10] K. Heimann, P. Gorczak, C. Bektas, F. Girke, C. Wietfeld, "Software-defined end-to-end evaluation platform for quality of service in non-standalone 5G systems", in: *IEEE International Systems*

- Conference (SysCon) , pp. 1–8, September, 2019.
- [11] S.M. Hussain, K.M. Yusof, R. Asuncion, S.A. Hussain, “Artificial intelligence based handover decision and network selection in heterogeneous internet of vehicles”, *Indonesia. J. Electr. Eng. Comput. Sci.* 22, 1124–1134, May, 2021.
- [12] K. Jellid, T. Mazri, “Comparative study on the protocols used by autonomous car, DSRC, C-V2X”, *Inf. Syst. Sec. 5G*. In Proceedings of the 4th International Conference on Networking, 1–8, April, 2021.
- [13] A.I. Károly, R. Fullér, P. Galambos, “Unsupervised clustering for deep learning: A tutorial survey”, *Acta Polytech. Hung.* 15, 29–53, Vol. 15, No. 8, 2018.
- [14] Z. Khan, P. Fan, F. Abbas, H. Chen, S. Fang, “Two-level cluster based routing scheme for 5G V2X communication”, *IEEE Access* 7, 16194–16205, January, 2019.
- [15] Q. Liu, C.F. Kwong, S. Zhang, L. Li, J. Wang, “A fuzzy-clustering based approach for MADM handover in 5G ultra-dense networks”, *Wirel. Netw.* 28, 965–978, September, 2019.
- [16] Kai Zhou and Tang Jiong. "Harnessing fuzzy neural network for gear fault diagnosis with limited data labels." *The International Journal of Advanced Manufacturing Technology* 115, no. 4 : 1005-1019, 2021.
- [17] G.R. MacCartney, T.S. Rappaport, “Rural macrocell path loss models for millimeter wave wireless communications”, *IEEE J. Select. Areas Commun.* 35, 1663–1677, April, 2017.
- [18] I. Mavromatis, A. Tassi, R.J. Piechocki, A. Nix, “Beam Alignment for Millimetre Wave Links with Motion Prediction of Autonomous Vehicles”, February, 2017.
- [19] M. Mezzavilla, M. Zhang, M. Polese, R. Ford, S. Dutta, S. Rangan, M. Zorzi, “End-to-end simulation of 5G mmWave networks”, *IEEE Commun. Surv. Tutorials* 20, 2237-2263, April, 2018.
- [20] J. Du, Y. Zhang, Y. Chen, X. Li, Y. Cheng and M.V. Rajesh, “Hybrid beamforming NOMA for mmWave half-duplex UAV relay-assisted B5G/6G IoT networks”. *Computer Communications*, 180, pp.232-242, December, 2021.
- [21] G. Pocovi, M. Lauridsen, B. Soret, K. I. Pedersen, and P. Mogensen, “Automation for on-road vehicles: Use cases and requirements for radio design”, In 2015 IEEE 82nd Vehicular Technology Conference (VTC2015-Fall), pp. 1-5. IEEE, January, 2015.
- [22] S.B. Prathiba, Raja, G. Raja, A.K. Bashir, A.A. AlZubi, and B. Gupta, “SDN-assisted safety message dissemination framework for vehicular critical energy infrastructure”, *IEEE Transactions on Industrial Informatics*, 18(5), pp.3510-3518, September, 2021.
- [23] T.S. Rappaport., Y. Xing, O. Kanhere, S. Ju, A. Madanayake, S. Mandal, A. Alkhateeb, and G.C. Trichopoulos, “Wireless communications and applications above 100 GHz: Opportunities and challenges for 6G and beyond”. *IEEE access*, 7, pp.78729-78757, June, 2019.
- [24] J.R. Beulah, and D.S. Punithavathani, D., “A hybrid feature selection method for improved detection of wired/wireless network intrusions”, *Wireless Personal Communications*, 98(2), pp.1853-1869, September, 2018.
- [25] M.R. Palas, M.R. Islam, P. Roy, M.A. Razzaque, A. Alsanad, S.A. AlQahtani and M.M. Hassan, “Multi-criteria handover mobility management in 5G cellular network”, *Computer Communications*, 174, 81-91, June, 2021.
- [26] RK. Srinivasa, N.K.S. Naidu, S. Maheshwari, C. Bharathi, and H. Kumar, “Minimizing latency for 5G multimedia and V2X applications using mobile edge computing”, In 2019 2nd International Conference on Intelligent Communication and Computational Techniques (ICCT), pp. 213-217, September, 2019.
- [27] T. Shimizu, H. Lu, J. Kenney and S. Nakamura, “Comparison of DSRC and LTE-V2X PC5 mode 4 performance in high vehicle density scenarios”, In Proceedings of the ITS World Congress , pp. 1-7, October, 2019.
- [28] C.R. Storck and F. Duarte-Figueiredo, “A 5G V2X ecosystem providing internet of vehicles”. *Sensors*, 19(3), p.550, January, 2019.
- [29] M.N. Tahir and M. Katz, “Performance evaluation of IEEE 802.11 p, LTE and 5G in connected vehicles for cooperative awareness”. *Engineering Reports*, 4(4), p.e12467, October, 2021.
- [30] M.N. Tahir and M. Katz, “ITS Performance Evaluation in Direct Short-Range Communication (IEEE 802.11 p) and Cellular Network (5G)(TCP vs UDP)”, In *Towards Connected and Autonomous Vehicle Highways* Springer, Cham, pp. 257-279, 2021.
- [31] M.A. Ullah, R. Keshavarz, M. Abolhasan, J. Lipman, K.P. Esselle and N. Shariati, “A Review on

Antenna Technologies for Ambient RF Energy Harvesting and Wireless Power Transfer: Designs, Challenges and Applications”, IEEE Access, February, 2022.

- [32] Online accessed: Jan. 2022. ETSI TS 122 185 v15.0.0. https://www.etsi.org/deliver/etsi_ts/122100_122199/122185/15.00.00_60/ts_122185v150000p.pdf
- [33] Z. Wu, Y. Xiong, S.X. Yu and D. Lin, “Unsupervised feature learning via non-parametric instance discrimination”, In Proceedings of the IEEE conference on computer vision and pattern recognition, pp. 3733-3742, 2018.
- [34] J. Zhao, Y. Liu, C. Wang, L. Xiong and L. Fan, “High-speed based adaptive beamforming handover scheme in LTE-R”, IET Communications, 12(10), pp.1215-1222, May, 2018.
- [35] L. Zhao, J. Fang, J. Hu, Y. Li, L. Lin, Y. Shi and C. Li., “The performance comparison of LTE-V2X and IEEE 802.11 p”, In 2018 IEEE 87th Vehicular Technology Conference (VTC Spring), pp. 1-5, June, 2018.
- [36] J.S.R. Jang., “ANFIS : Adaptive-Ne twork-Based Fuzzy Inference System” , IEEE Transactions On Systems, Man, and Cybernetics, Vol. 23, No. 3, pp. 665-685, 1993.
- [37] online accessed: Feb. 2022. MathWorks. Fuzzy logic toolbox user’s guide. Natick: Inc, 3, Apple Hill Drive; p. 137–179. <https://person.dibris.unige.it/masulli-francesco/lectures/ML-CI/lectures/MATLAB%20fuzzy%20toolbox.pdf>.
- [38] A. Dayal, E. Colbert, V. Marojevic and J. Reed, “Risk controlled beacon transmission in v2v communications”, In 2019 IEEE 89th Vehicular Technology Conference (VTC2019-Spring) (pp. 1-6). IEEE, April, 2019.
- [39] L. Montero, C. Ballesteros, C. De Marco, L. Jofre, “Beam management for vehicle-to-vehicle (V2V) communications in millimeter wave 5G”, Veh. Commun. 34, 100424, April, 2022.
- [40] E. Skondras, A. Michalas, D.J. Vergados, E.T. Michailidis, and N.I. Miridakis, A Network Slicing Algorithm for 5G Vehicular Networks. In 2021 12th International Conference on Information, Intelligence, Systems & Applications (IISA), pp. 1-7, July, 2021.
- [41] Weijun Xing, Wang Ning, Wang Chao, Liu Fuqiang, and Ji.Yusheng, "Resource allocation schemes for D2D communication used in VANETs." In 2014 IEEE 80th vehicular technology conference (VTC2014-Fall), pp. 1-6. IEEE, 2014.
- [42] Hamdy A.M. Sayedahmed, Emad M. Elgamal, Hesham A. Hefny. F-802.11p: a fuzzy enhancement for IEEE 802.11p in vehicle-to-everything communications. International Journal of Computer Networks and Communications (IJCNC), volume 14, issue 4, pages 19 – 40, July 2022.
- [43] Mary amAbdulazeez-Ahmed, Nor Kamariah Nordin, Aduwati Bint Sali and Fazirulhisyam Hashim, "Multi-Criteria Handover Decision for Heterogeneous Networks: Carrier Aggregation Deployment Scenario." International Journal of Computer Networks & Communications (IJCNC), volume 12, issue 4, page 41-54, July 2020.